Multifrequency Microwave Emission From the Dome-C Area on the East Antarctic Plateau: Temporal and Spatial Variability

Giovanni Macelloni, *Member, IEEE*, Marco Brogioni, *Student Member, IEEE*, Paolo Pampaloni, *Fellow, IEEE*, and Anselmo Cagnati

***Abstract*—The Antarctic plateau that extends for several hundred kilometers with an average altitude of close to 3000 m a.s.l. is the highest part of the east Antarctic ice cap. This area provides unique opportunities for various scientific disciplines, including glaciology and atmospheric and earth sciences. In addition, there is growing interest in using the Antarctic plateau, for calibrating and validating data of satellite-borne microwave radiometers, thanks to the size, structure, and spatial homogeneity of this area, and the thermal stability of deeper snow layers. In this paper, we analyze the temporal and spatial variabilities of multifrequency microwave emission from the area surrounding the Dome-C scientific station using Advanced Microwave Scanning Radiometer data collected throughout 2005. Moreover, a multilayer coherent electromagnetic model is used for estimating the contribution of snow layers to emission at various frequencies. The results are consistent with the physical structure of the ice sheet and with its seasonal and spatial variations.**

***Index Terms*—Advanced Microwave Scanning Radiometer-EOS (AMSR-E), Antarctica, electromagnetic models, microwave radiometry.**

I. Introduction

ANTARCTICA is the coldest place on Earth. Temperatures reach a minimum of between −85 °C and −90 °C in the winter and about 50° higher during the summer months. Some 95% of Antarctica is covered by an ice cap (which contains about 90% of all ice existing in the world) that averages 1.6 km in thickness and is characterized by a high surface albedo that reflects 80%–90% of the solar radiation, leaving little energy to heat the surface in summer. Snow cover, which is a key component in the global hydrological cycle, strongly influences the overlying atmosphere and, hence, the polar and global climate.

Several studies of Antarctica using satellite-borne microwave radiometers have been performed since the launching of the Scanning Microwave Spectrometer (SCAMS) in 1975 and have continued with the Scanning Multichannel Microwave Radiometer (SMMR), the Special Sensor Microwave/Imager Radiometer (SSM/I), and the Advanced Microwave Scanning Radiometer-EOS (AMSR-E) [1]–[5]. These studies focused on analyzing spatial and temporal variations of microwave signatures on a continental scale and relating them to both topographical and morphological structures of the ice sheet surface as well as how they change over time. One of the first papers [1] correlated snow particle size with observed emissivity and used these data to calculate accumulation rates in selected areas. The temporal and spatial variability of brightness temperature (Tb) at 37 GHz was analyzed in [7] and [8] and related to variation in snow surface temperature. Still, other works [9], [10] addressed the development of a radiative transfer model to relate the variation in multifrequency microwave emission, which was measured by a satellite sensor, to the variation that occurred in snow temperature at different depths.

Moreover, these investigations showed that the mean annual variability of Tb decreases when the frequency decreases. At Ka-band (37 GHz), this variability was about 50 K (corresponding to the average annual air temperature variation), while at C-band (6.9 GHz), it was only about 5 K. By using a polynomial fit extrapolated from the measurements, the variability at L-band (1.4 GHz) was estimated to be much lower than 1 K in [6]. Model simulations carried out in the same paper confirmed this value. These radiometric time series showed lagged seasonal Tb increasing with wavelength. Indeed, previous analyses carried out in the Dome-C area showed that the time delay between air temperature (measured by Automatic Weather Station) and microwave Tb was about 15 days at 37 GHz, 28 days at 18 GHz, and was higher than 30 days at 6.9 and 10 GHz, although an exact estimate could not be made clearly [9], [10]. This lag implies a frequency-dependent depth weighting of thermal emission, which also depends on the physical properties of snow. The spectral response and polarization differences also vary as a function of season.

Missions based on L-band radiometers such as the European Space Agency's Soil Moisture and Ocean Salinity mission (SMOS) and NASA's Aquarius are planned for the near future. In an attempt to use the Antarctic plateau in validating and calibrating data from these missions, an experimental campaign called DOMEX took place in the Austral summer of 2004–2005 at the Italian–French station of Concordia (located at Dome-C

Manuscript received June 1, 2006; revised December 6, 2006. This work was supported in part by the European Space Agency under Contract 18060/04/NL/CB and in part by the National Programme of Antarctic Research under Project 2004/3.01.

G. Macelloni, M. Brogioni, and P. Pampaloni are with the Istituto di Fisica Applicata "Nello Carrara," Consiglio Nazionale delle Ricerche, 50019 Sesto Fiorentino, Italy (e-mail: G.Macelloni@ifac.cnr.it; M.Brogioni@ifac.cnr.it; P.Pampaloni@ifac.cnr.it).

A. Cagnati is with the Centro Valanghe di Arabba, Agenzia Regionale per la Prevenzione e Protezione Ambientale del Veneto, 32020 Arabba di Livinallongo, Italy (e-mail: acagnati@arpa.veneto.it).

Digital Object Identifier 10.1109/TGRS.2007.890805

in the east Antarctic plateau). The DOMEX campaign also included a series of conventional snow measurements that were carried out at different times in several places around the base. The results of DOMEX were recently presented in [11].

Compared with other possible targets, the area near the base of Concordia appears to be particularly suited for this purpose. In fact, the site, which is located more than 1000 km from the coast, is spatially homogeneous at a hundred kilometer scale and offers extremely small surface slopes. Roughness is more limited than in other Antarctic areas [12], and the amplitude of seasonal fluctuations in the firn temperature decreases with depth up to 15 m [13]. Moreover, atmospheric conditions are very clear for most of the year, and precipitations are limited.

In addition to its usefulness in calibrating microwave sensors, recent studies demonstrate that the high stability of ground reflectance makes this area well suited as a calibration site for optical satellites [14], [15]. In summary, the site's unique characteristics, joined with detailed information obtained from several past campaigns (e.g., bedrock and snow topography, snow accumulation rate, etc.) as well as several instruments developed *in situ* for continuous atmospheric and snow measurements, make this area very attractive for the calibration of any remote sensing mission.

In this paper, following a short description of the test site, we analyze the snow data and the temporal and spatial variability of multifrequency microwave emission from the area around Dome-C by using multifrequency data collected by AQUA/AMSR-E in 2005. Microwave data, gathered over a restricted area (60 $\times$ 90 km), were related to the physical temperature of the ice sheet measured at different depths. An analysis was then performed on a larger area (250 $\times$ 250 km) in an attempt to identify the most homogenous part of the area (i.e., where the microwave signal remains more stable in time and space) for use as calibration target. Although satellite L-band data are not yet available, the data collected at higher frequencies, combined with an electromagnetic model able to simulate microwave emission, could provide useful indications about the stability of emission at this band. In the last part of this paper, a multilayer coherent electromagnetic model employing snow parameters measured during DOMEX as input was used to estimate the contribution of snow layers to emission at various frequencies.

II. Test Site and Experimental Data

The Antarctic plateau, that extends for several hundred kilometers with an average altitude of close to 3000 m a.s.l. and a peak of 4200 m, is the highest part of the east Antarctic ice cap.

The Italian–French base of Concordia is located at Dome-C in the middle of the east Antarctic plateau at $75^\circ\ 06'06''$ S, $123^\circ\ 23'42''$ E, and at an altitude of 3280 m a.s.l. It is about 1100 km from the French coastal base of Dumont D'Urville and 1200 km inland from the Italian base, the Mario Zucchelli Station (Fig. 1). The location of the base was originally selected for glaciological purposes, since 3000 m of layered ice has a great potential for long-time paleoclimatic reconstruction. The European Programme for Ice Coring in Antarctica (EPICA) has been able to reconstruct the history of the climatic and environmental changes for the last 800 000 years [16]. Moreover, the site provides unique opportunities for various scientific fields including glaciology, atmospheric and earth sciences, astronomy, and astrophysics.

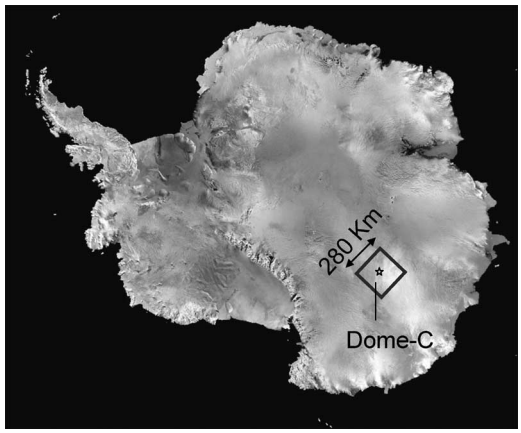

Fig. 1. Dome-C, Antarctica. The star represents the location of the Concordia station at the top of the dome. The square area (around 280 $\times$ 310 km) represents the area where the spatial satellite analysis was performed.

The annual mean air temperature is -50.8 °C, while the mean winter (from June to August) and summer (from December to February) temperatures are -60 °C and -30 °C, respectively. Annual (solid) precipitation is of the order of 30–40 mm (snow water equivalent), which, for a typical sublimation of 10%–20%, leads to an annual accumulation of about 25–35 mm (snow water equivalent) [17]–[19].

This site is well-suited for calibration of microwave sensors for several reasons: first, it can be viewed on a sub-daily basis by polar-orbiting satellites at a variety of incidence and azimuth angles; the snow surface is relatively homogeneous at the 100 km scale; surface roughness is minimal compared to other ice sheet locations; environmental conditions, which influence Tb, are well-documented by an Automatic Weather Station that provides barometric pressure, air temperature, wind speed and direction.

The AMSR-E is a multifrequency dual-polarized radiometer flying in a polar orbit at an altitude of 705 km and can be successfully exploited for global and regional investigations of the Earth's surface. This instrument, which was developed by the Japan Aerospace Exploration Agency (JAXA) for the NASA AQUA satellite, explores the Earth's surface with an angular scan at an incidence angle of 54.8° and a swath of 1445 km. The frequency range extends from 6.9 to 89 GHz, which is subdivided into six channels with a corresponding ground resolution (3-dB footprint) ranging from 74 $\times$ 43 km at the lower frequency to 6 $\times$ 4 km at 89 GHz. Sensitivity varies from 0.3 K at 6.9 GHz (2.6-ms integration time) to 1.1 K (1.3-ms integration time) at 89 GHz. Global swath calibrated brightness temperature data, resampled at average resolutions of 56, 38, 21, 12, and 5.4 km, are delivered by the National Snow and Ice Data Center. The radiometric data used in this study were collected in 2005 over an area of about 280 $\times$ 310 km surrounding the Concordia station. The analysis was performed at both vertical and horizontal polarizations, and both presented similar trends. However, the horizontal component of Tb was

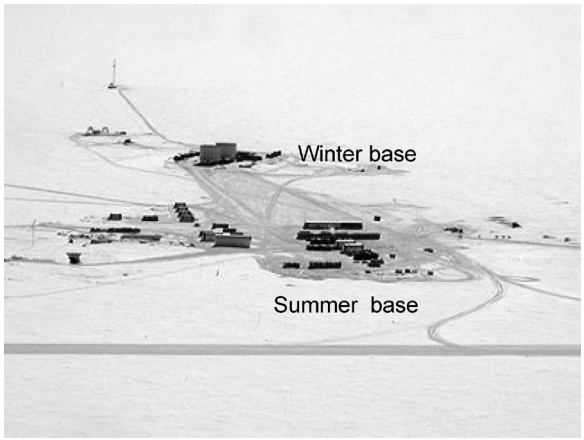

Fig. 2. Aerial view of the Concordia station layout.

noisier compared to the vertical one as observed in previous papers [9], [10], and while some results are presented at both polarizations, this paper deals mainly with the results obtained at V polarization.

The physical parameters of snow, down to 10 m below the surface, were investigated in December 2005 during the DOMEX experiment [11] with conventional snow measurements [20], which were carried out in several pits dug in the area surrounding the base (Fig. 2). A 4-m-deep pit and four 1-m-deep pits were excavated in different places to test the homogeneity of the area on a scale of 1 km^2. In addition, a 10-m-deep (diameter of 10 cm) ice core was drilled, and the main characteristics of the ice were measured. The data presented in this paper have been obtained from the snow pit up in the first 4 m and from the ice core in the 4- to 10-m range. These measurements served as a way to obtain an accurate description of the snow layering by identifying the following quantities for each layer: temperature, height, density, hardness, grain shape and size, and dielectric constant. The first quantities were measured using conventional methods, while the dielectric constant was measured using a commercial electromagnetic probe. The probe, which is designed to operate in extreme conditions between 500 and 900 MHz, measured the resonant frequency and the 3-dB bandwidth, making it possible to compute the complex dielectric constant of snow. The snow density was derived from this quantity using semi-empirical formulas.

Grain size and shape were first estimated on site by visual interpretation, carried out by a snow expert using an optical lens with 0.1-mm reference. Moreover, digital photos were taken to verify the results. It should be noted that, although the measurement of grain shape and size is generally a difficult task, due to the intrinsic variability of grains, the shapes of the grains observed in the Antarctic plateau were more regular (in most cases spherical or subspherical) than those observed in other regions.

Snow temperature was also monitored by means of a thermal infrared (Tir) sensor during DOMEX and by a string of thermistors placed into the snowpack at different depths down to 10 m below the surface for the entire year. The probes in the first 100 cm were embedded in snow, while the others were

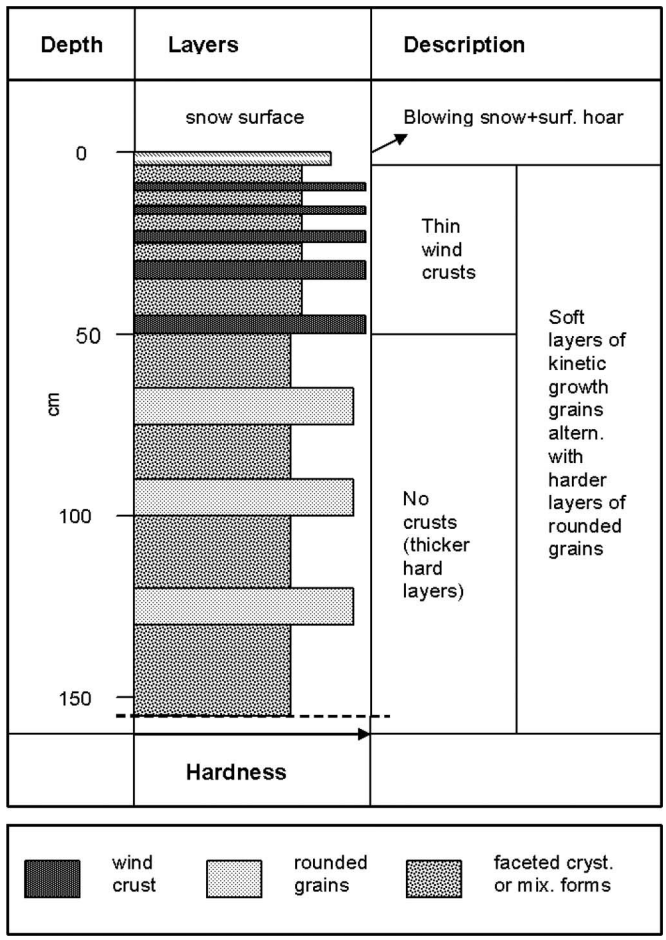

Fig. 3. Schematic diagram of the snow structure (layer thickness and hardness are not in scale).

placed into an already existing hole. The latter was sealed to guarantee thermal equilibrium with the snowpack, which was reached a few hours following closure. The probes were PT100 (DIN-A), the resolution was 0.02 °C, and the accuracy was 0.30 °C within the −100 °C–0 °C range; they were calibrated prior the DOMEX campaign by the manufacturer (information on the probes and data logger is available at http://www.lsi-lastem.it/). Temperature data were continuously recorded by a data logger on an hourly time basis. Thanks to a researcher who remained at the Concordia station throughout the winter, the valuable snow temperature measurements were continued during the 2005 and 2006 austral autumn and winter seasons.

III. Experimental Results

A. Snow Measurements

The snowpack at Dome-C, as observed during the 2004–2005 summer throughout the DOMEX experiment, was a succession of soft layers consisting of kinetic growth grains alternating with harder layers of rounded grains. In the upper part of the profiles (generally down to a depth of 50 cm), the hard layers often had the typical appearance of wind crusts (very hard, with thickness values ranging from 0.5 to 1 cm) (Fig. 3). At greater depths, the crusts tended to disappear, and the hard layers were thicker and made of larger grains. In

general, the kinetic reconstruction activity of the grains was evident along all profiles. This was due to the thermal gradient, which, even if not particularly large, acted continuously over time. The water vapor flux was partially blocked by the presence of hard layers where larger grains were usually found. The reconstruction, which led to the formation of large faceted crystals, was active throughout the year, except during periods in which the thermal gradient was reversed (end of February and end of September) and when the snowpack was in quasi-isothermal conditions. According to the International Association of Hydrological Sciences (IAHS) classification [20], the kinetic reconstruction grains could be ascribed to mixed shapes (subclass 4c) measuring from 0.7 to 1.5 mm or to faceted crystals (subclass 4a) that could measure as much as 2.5–3 mm. These typologies of grains clearly predominated along all the profiles examined and lent the snowpack an incoherent appearance. The surface hoar (subclass 7a), which was almost always present on the snowpack surface, measured about 0.5 mm. Instead, wind crusts (subclass 9d) were generally made up of small rounded grains with dimensions of about 0.2–0.3 mm, whereas in layers formed by rounded grains (subclasses 3a and 3b), grain size tended to increase to a maximum of 0.7 mm. Although cases of discontinuity existed, due to the succession of layers having different characteristics, grain size generally increased at greater depths.

Snow density changed according to the characteristics of the layers and, in particular, depending on the typology of grains that made up the layers. As a result, the trend was rather discontinuous, particularly in the first meter. Data showed layers composed of faceted crystals or mixed shapes with a density varying from about 300 to 410 kg/m^3 as a function of depth (with minimum values of 260 kg/m^3), whereas the layers composed of rounded grains had higher densities, which ranged from 370 to 510 kg/m^3 depending on depth (with maximum values of 520 kg/m^3). On average, snow density increased with depth, although the densifying process was rather low in the first 4 m and changed from 360 kg/m^3 in the first meter to 390 kg/m^3 in the fourth meter, reaching 480 kg/m^3 at 8–10 m. Clearly, the process of kinetic reconstruction leading to the formation of large highly porous grains prevailed with respect to the evolution toward equilibrium forms and to the compacting action of wind. This gave a rather low cohesion to the snowpack in the relatively deep layers as well.

The average values of grain size (i.e., the maximum dimension of the prevalent grain for each layer) and density as a function of depth in the first 10 m are represented in Fig. 4. The real part of the dielectric constant showed values between 1.4 and 1.85 (typical for dry snow in this density range), and the derived snow density values were in good agreement with those directly measured using the conventional method. This quantity is also represented in Fig. 4, where we can note a good agreement between both measurements. The computed root-mean-square error (rmse) is 45 kg/m^3. Differences were probably due to the fact that the volume sampled by the probes was different (i.e., the volume sampled by the probe was bigger than the area analyzed with the manual sampler). Snow temperature measurements collected from January 2005 to December 2005 down to 10 m below the surface are represented in Fig. 5. The data show that, at a depth of 10 m, the temperature was stable in time, the mean annual value was −54.5 °C, and the standard deviation was 0.2 °C. Nevertheless, conditions were already quasi-isothermal at a depth of 6 m, showing a variation over the year of around 3 °C. Moreover, the ice pack down to 1.5 m was in quasi-isothermal condition from May to October (the total variation in time and depth along this period was about 5 °C). Seasonal variations were particularly evident in the first 4 m, where the differences between surface and 4-m-deep temperatures could exceed 25 °C. The thermal gradient was negative during the spring and part of the summer, while it was positive during the rest of the year. Surface temperatures varied from maximum values of −20 °C/−22 °C in November and December to minimum values of −68 °C/−70 °C, which were reached in April. Daily

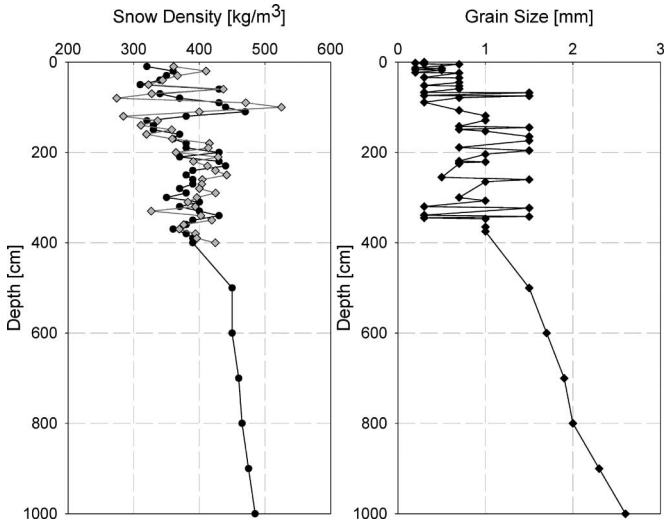

Fig. 4. (Left) Average values of snow density measured by the snow sampler (black) and electromagnetic probe (gray) as a function of depth in the first 10 m (4 m for the probe). (Right) Measured grain size (i.e., the maximum dimension of the prevalent grain for each layer) as a function of depth in the first 10 m.

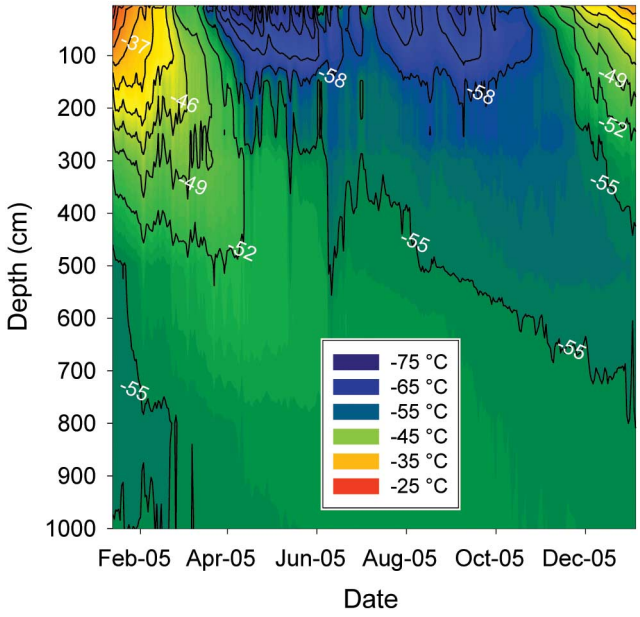

Fig. 5. Snow temperature in the first 10 m as a function of time.

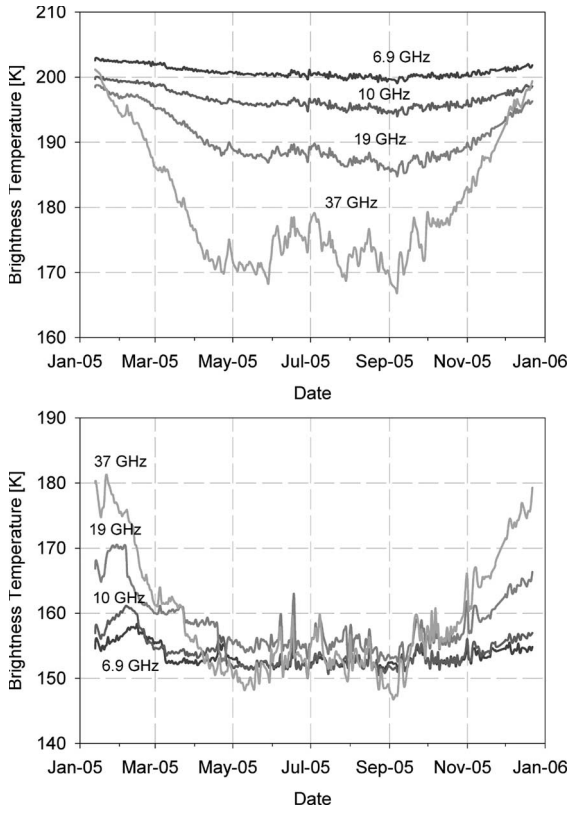

Fig. 6. Tb at (top) V and (bottom) H polarizations measured from AMSR-E as a function of time.

variations occurred only at a depth of 20–30 cm during spring and summer, coinciding with significant variations in the air temperature.

B. Satellite Measurements: Time Variability

The temporal variability of Tb was analyzed by using AMSR-E data collected in 2005 over an area of about 60 × 90 km around Dome-C (corresponding to a 3 × 3 pixel grid at C-band centered at the Concordia base) and through *in situ* measurements of snow parameters carried out at different depths down to 10 m below the surface. The analysis was conducted on a great number of images (a total of 1950 images, and at least five images per day); the mean value of the 3 × 3 pixel area was extracted from each image and then averaged daily to reduce noise. Fig. 6 shows the vertical and horizontal component of Tb as a function of time for all the AMSR-E frequencies taken into consideration. We can see that Tb at C-band (6.9 GHz) and X-band (10 GHz) changed regularly following the yearly cycle with a maximum variation of about 4 and 6 K at V polarization and 7.5 and 11 K at H polarization, respectively. The variation increased at Ku-band (19 GHz) and Ka-band (37 GHz), showing significant fluctuations (already observed in an other paper [10]), especially in April, May, and September. From this figure, we can also observe that, as expected, the horizontal polarization was noisier compared to the vertical one. Moreover, strange abrupt transitions were observed at H polarization in the beginning of the year (from January to March), which did not seem related to changes in emission (no changes were recorded at V polarization and in air and snow temperature at the same time) but to a malfunctioning of the sensor. For example, from January 20 to January 21, Tb increased to 4 K at Ka-band and 2 K at Ku-band; from February 6 to February 7, Tb decreased to 4 K at Ku-band; or from March 8 to March 9, Tb decreased to 2 K at C-band. This could also be emphasized in Fig. 7, where the annual trend of the Polarization Index (PI) defined as $\mathrm{PI} = (T_{\mathrm{bv}} - T_{\mathrm{bh}})/(0.5^{*}(T_{\mathrm{bv}} + T_{\mathrm{bh}}))$ is represented for all the frequencies. In fact, although snow stratification can have a different impact on the two polarizations, rapid variations between H and V polarizations are unexpected in Antarctica, and the monitoring of PI can be a simple method to check data anomalies.

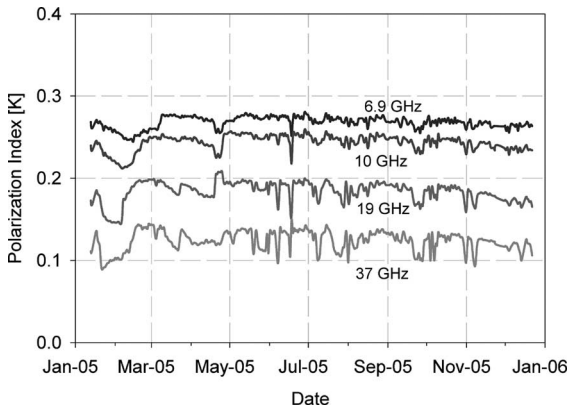

Fig. 7. $\mathrm{PI} = 2(T_{\mathrm{bv}} - T_{\mathrm{bh}})/(T_{\mathrm{bv}} + T_{\mathrm{bh}})$ measured from AMSR-E as a function of time.

From the figure, we can note that the PI decreased with frequency and that, at each frequency, its mean value remained almost constant during the year, while rapid fluctuation corresponds to possible anomalies observed at H polarization.

In comparing Tb with the air and snow temperature measured at different depths (Fig. 8), we see that lower frequencies were correlated to the temperature in the deeper layers, which changed regularly according to seasons, while the emission in Ku-band and Ka-band closely followed the temperature in the upper layers with steep variations in the mid seasons (December–April and October–December) and fairly strong fluctuations during the Austral winter. This fact is more evident in Fig. 9, which directly compares Tb at 37-GHz band with the temperature of a layer of snow 50 cm below the surface and Tb at 19-GHz band with the snow temperature measured 200 cm below the surface. Even if there are some differences between satellite and *in situ* data (particularly at the beginning of the year), it can be noted that, especially at 37 GHz, the microwave signal was able to follow the slight changes occurring in snow temperature.

In this comparison, it is important to point out that, although the daily average of satellite and snow temperatures was computed using measurements collected at different times (i.e., the number of satellite data per day was lower than the number of snow temperature data), the asynchrony in data collection was not relevant. Indeed, the daily variation in snow temperature measured down to 50 cm was very small. For example, the daily standard deviation of temperatures measured at −50 and −300 cm for the whole year was 0.3 °C and 0.2 °C, respectively.

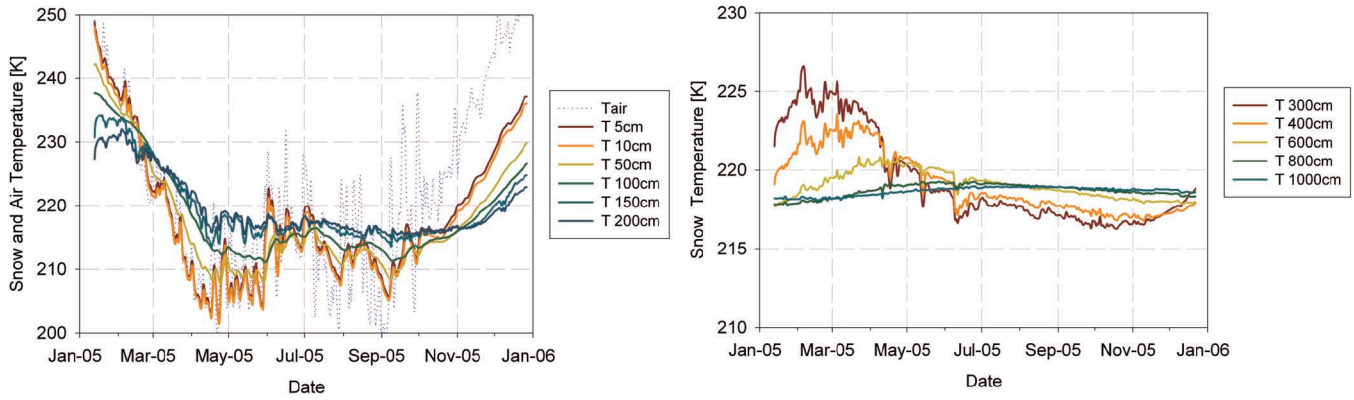

Fig. 8. Air and snow temperatures measured at different depths in the first 10 m along the year 2005. (Left) From air to 200 cm. (Right) From 300 to 1000 cm.

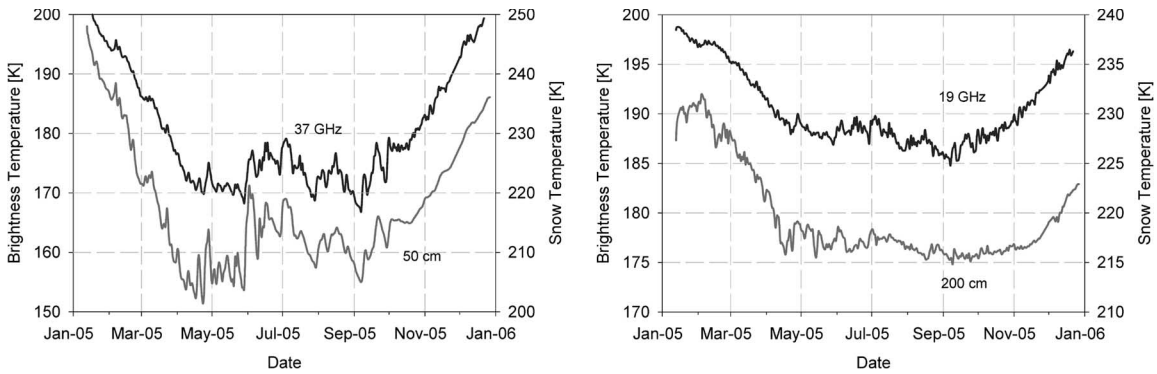

Fig. 9. Tb at (left) 37 GHz and (right) 19 GHz as a function of time compared, respectively, with snow temperature at −50 and −200 cm from the surface.

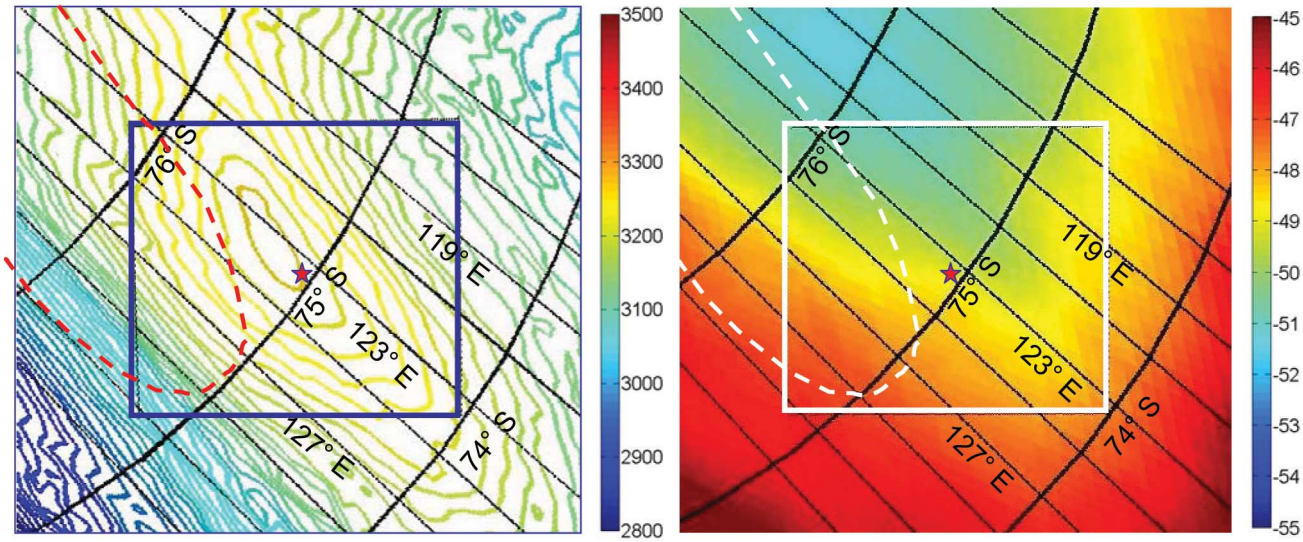

Fig. 10. Location of the Dome-C area. (Left) Surface topography. Isolines are every 10 m from 2000 to 3500 m [21]. (Right) Mean annual surface temperature from −55 °C to −45 °C [22]. The star indicates the location of the Concordia base. The highlighted square box indicates the area in which the AMSR-E analysis was performed. The megadunes area is indicated in dashed line and is derived from [23].

A direct comparison of two data sets showed very high correlations, with determination coefficients R^2 (37 GHz) = 0.98 and R^2 (19 GHz) = 0.90.

C. Satellite Data: Spatial Variability

The spatial variability at different times was analyzed by using data acquired in a 280 × 310 km area centered at the Concordia base (corresponding to a 25 × 25 pixel grid observed by the 3-dB footprint at C-band). In this case, images were selected from a single AMSR-E orbit (i.e., all the images were chosen from a single swath and with the same equator crossing time) to guarantee the same geometry of the observed area and to simplify the coregistration process; since the revisit time of the AMSR-E orbit is 16 days, 22 images were taken into consideration for the period of one year. In Fig. 10, the

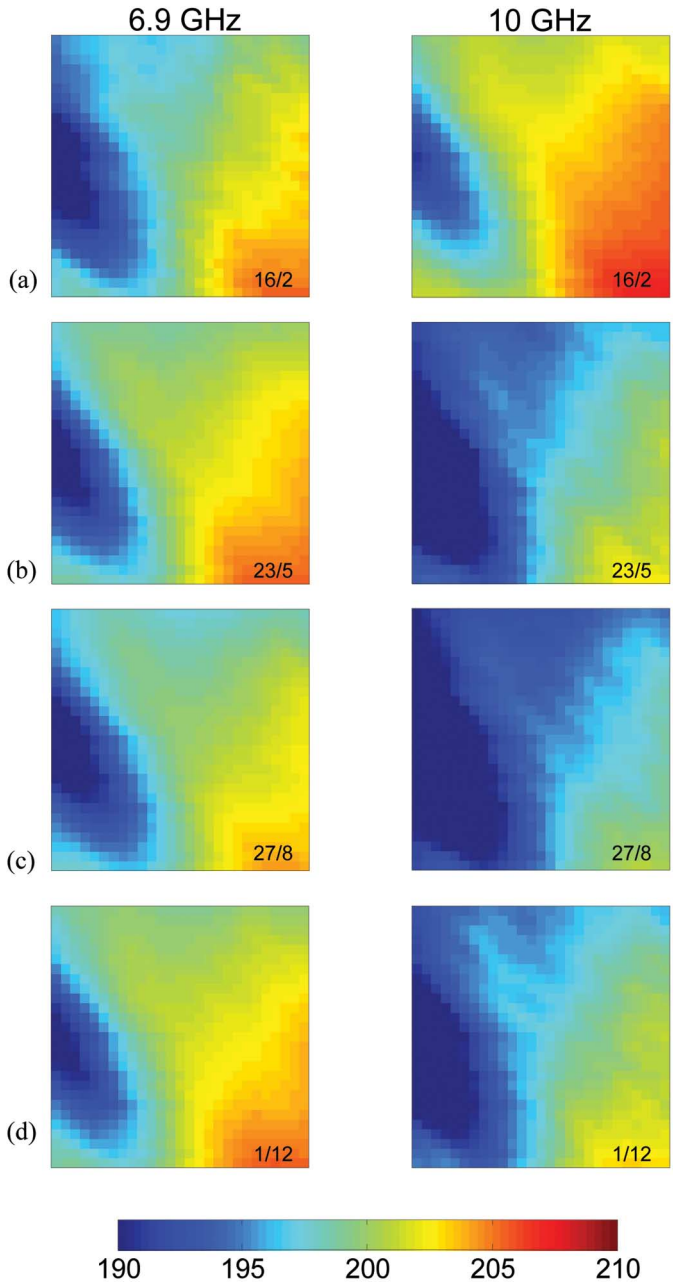

Fig. 11. AMSR-E data at 6.9 and 10 GHz collected over a 280 × 310 km area (25 × 25 pixel) centered at the Concordia base in (a) February, (b) May, (c) August, and (d) December 2005.

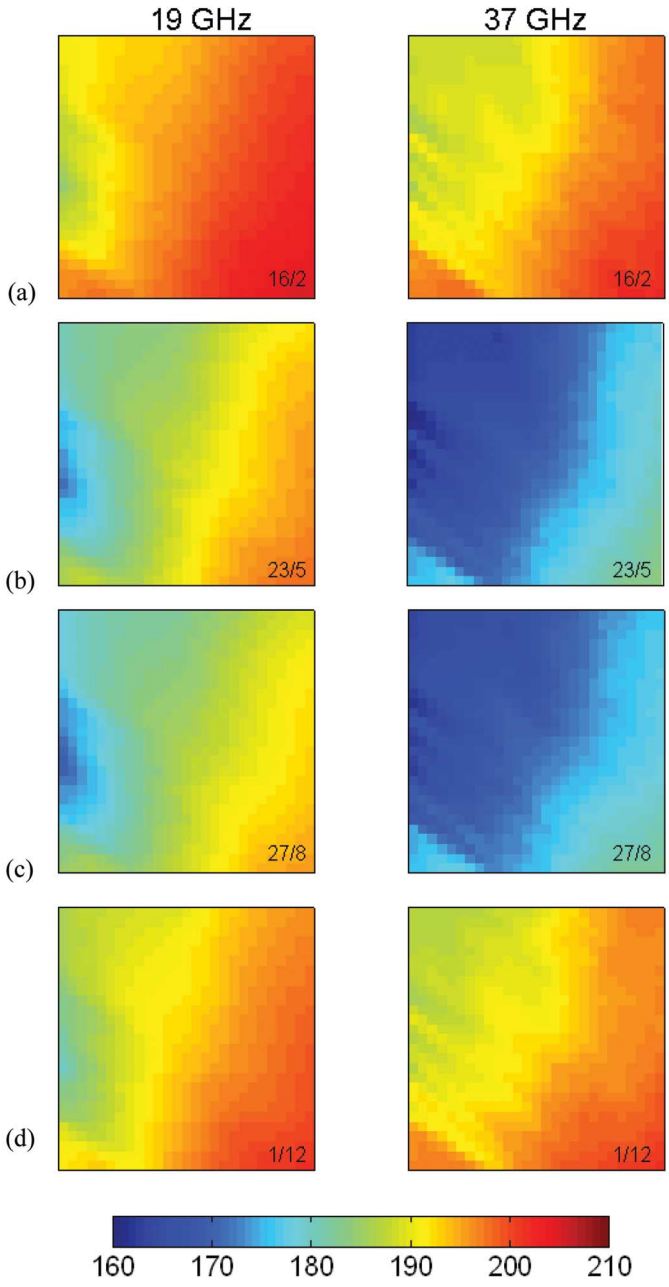

Fig. 12. AMSR-E data at 19 and 37 GHz collected in a 280 × 310 km area (25 × 25 pixel) centered at the Concordia base in (a) February, (b) May, (c) August, and (d) December 2005.

topography and mean annual temperature maps of the Dome-C area were represented (data were derived from [21] and [22]). The star indicates the position of the Concordia base, the square is the area in which the AMSR-E analysis was performed, and the dashed line points out the megadunes area as derived from [23]. Tb maps obtained from AMSR-E during the four seasons of the year (February, May, August, and December 2005) at 6.9, 10, 19, and 37 GHz V polarization in this area are represented in Figs. 11 and 12. We can see that, on each date, Tb at the highest frequencies (19- and 37-GHz band) decreased when the latitude increased, depending on the variation in air and surface snow temperatures and differences in the snow structure, with a maximum variation in summer from 160 to 210 K. In addition, the variation over time (from winter to autumn) was perfectly consistent with the seasonal temperature cycle and was similar to the variations measured in the smaller area (3 × 3 pixels) close to Dome-C, where the temporal variation was investigated. At lower frequencies, Tb presented similar spatial trends, but it had a much smaller variation (especially at C-band) in both space (20 K at C-band) and time. Indeed, radiation at this frequency is emitted by deeper layers that are much less affected by seasonal changes. At this frequency, it was possible to identify several features in the images that remained constant throughout the year and that were related not only to the variations in snow temperature at different depths but to the morphology and different physical properties of snow. For example, the blue area on the left side of the images corresponds to the region of the megadunes as

observed by Frezzotti *et al.* [17]. The megadunes cover an area of the east Antarctic plateau of around 500 000 km^2. Created over centuries of nearly continuous winds, megadunes have a height of few meters (1–8 m) and a length of 2–6 km (crest to crest). As shown in [21] and confirmed by the analysis of our data, the megadunes area presents an anomalous signature at all frequencies and both polarizations. In fact, the brightness temperature of this area is much lower than other parts in the image and was not caused by a difference in surface or subsurface temperature of the ice sheet as measured by thermal infrared sensor [8], [22] or shallow cores [24].

This effect could be explained by the presence of coarse grains in the firn that determines an increase in volume scattering and, consequently, a decrease of emission, as demonstrated by measurements and models analysis [25], [10].

The time variance computed in each pixel of the images confirmed the same trend. As an example, Fig. 13 shows the annual standard deviation at 6.9 GHz. It is interesting to note that the Tb variation was low throughout the image (less than 1 K in the largest portion) and that the maximum variation (1.6 K) was in the colder part of the region. From our analysis of the C-band images, we could also observe that the upper central part of the area was the most stable in time and the one recommended for use as an extended reference target for the calibration of satellite sensors, as highlighted in Fig. 13.

IV. Model Analysis

To analyze the experimental data and to estimate the snow layers that contributed most to the emission at a certain frequency, a physically based multilayer electromagnetic model based on previously documented models [6], [27]–[29] was developed. The snowpack was modeled as a stack of n layers with planar boundaries over a half-space medium. Each layer was considered as a collection of spherical ice particles embedded in air and characterized by its temperature, thickness, density, and permittivity. The permittivity of these particles was computed using a semi-empirical formula derived from the literature [32], [33]. The effective permittivity of the resulting medium was computed in accordance with the Strong Fluctuation Theory. The reflection and transmission waves in the layered medium were computed following the wave approach [30], and the contributions of the single snow layers to total brightness temperature were added by means of the fluctuation dissipation theorem [34].

All data used as inputs to the model in the first 10 m were taken or derived from ground measurements during DOMEX. Below this depth, the values were derived from EPICA drilling core [7] and glaciological models [26]. The snow temperature below 10 m was assumed to be constant at $-54.5\ ^\circ$C.

The grain radius in each layer was derived from experimental data up to 10 m (from DOMEX data set) and, using a glaciological model down to this depth, assumed the following growth law:

$$r(z) = \sqrt{r_0^2 + \frac{K_{\mathrm{growth}} \cdot z}{\pi \cdot D}}$$

where K_{growth} is the crystal growth rate (the typical value is 0.00042 mm^2/year), z is the snow depth, D is the mean annual thickness of the layer, and r_0 is the initial value [26]. The latter parameter was varied to best fit the experimental data and was found to be $r_0\ (0\ \mathrm{m}) = 0.04$ mm, $r_0\ (22\ \mathrm{m}) = 0.09$ mm, and $r_0\ (42\ \mathrm{m}) = 0.15$ mm.

A summary of the model input parameters used for the simulations is represented in Table I.

A comparison of model simulation performance over one year of AMSR-E data is represented in Fig. 14.

From the figure, we can note that, whereas the model well represents the general trends of the Tb, it slightly underestimates experimental values at 6.9 and 19 GHz, especially at the beginning of the season, and overestimates the measured Tb at 10 and 37 GHz for most of the annual cycle (with a maximum error of 5 K at 37 GHz). Moreover, the model was a little less sensitive to the Tb fluctuations observed in satellite data.

The small discrepancies between simulations and experimental data can be due to some approximations introduced in the model, which assumes spherical ice crystals and uniform plane interfaces between snow layers. Moreover, we presupposed temporal stability and spatial homogeneity of firn characteristics in the region investigated by the satellite radiometer (60 $\times$ 90 km), while snow data were collected in a more restricted area and in a limited time interval, except for temperatures.

In all cases, the R^2 determination coefficient of regressions between experimental and simulated data was very high. For example, it reached a value of 0.98 at 37 GHz and 0.96 at 19 GHz. The rmse values are 2.7 K at 37 GHz, 1.18 K at 19 GHz, 0.82 K at 10 GHz, and 0.73 K at 6.9 GHz.

The model was then used to compute the annual variation of Tb as a function of frequency. The results are shown in Fig. 15, which represents the yearly variation of the vertical component of Tb together with average values of experimental data (computed as the difference between maximum and minimum value) taken from 1978 to 2000 with SMMR and SSM/I and one year of AMSR-E data (2005).

We can see that model and data are in good agreement and that the expected annual variation in Tb at 1.4 GHz (derived from either data interpolation or model simulation) is very low (in the order of 0.5 K). This value is in accord with previous results [6] and confirms the interest in using the Antarctic plateau as a calibrator for low-frequency satellite radiometers.

Subsequently, the model was used to investigate the penetration of microwave radiation into the ice sheet as a function of frequency. Fig. 16 shows the contribution to the total emission of the layers included in the upper 100 m. The layer contributing 70% of the emission ranges from 50 m (at 6.9 GHz) to 4 m at the 37 GHz band. Moreover, at 37 GHz, no contribution to the emission is expected from layers below 20 m, whereas at lower frequencies, the depth of layers that contribute to emission increases and is greater than 100 m at C-band. The penetration depth computed according to the usual definition (power of electromagnetic field decays by a factor 1/e) is 2 m at 37 GHz, 5.5 m at 19 GHz, 13.2 m at 10 GHz, and 21 m at 6.9 GHz. These values are in good agreement with those computed in the

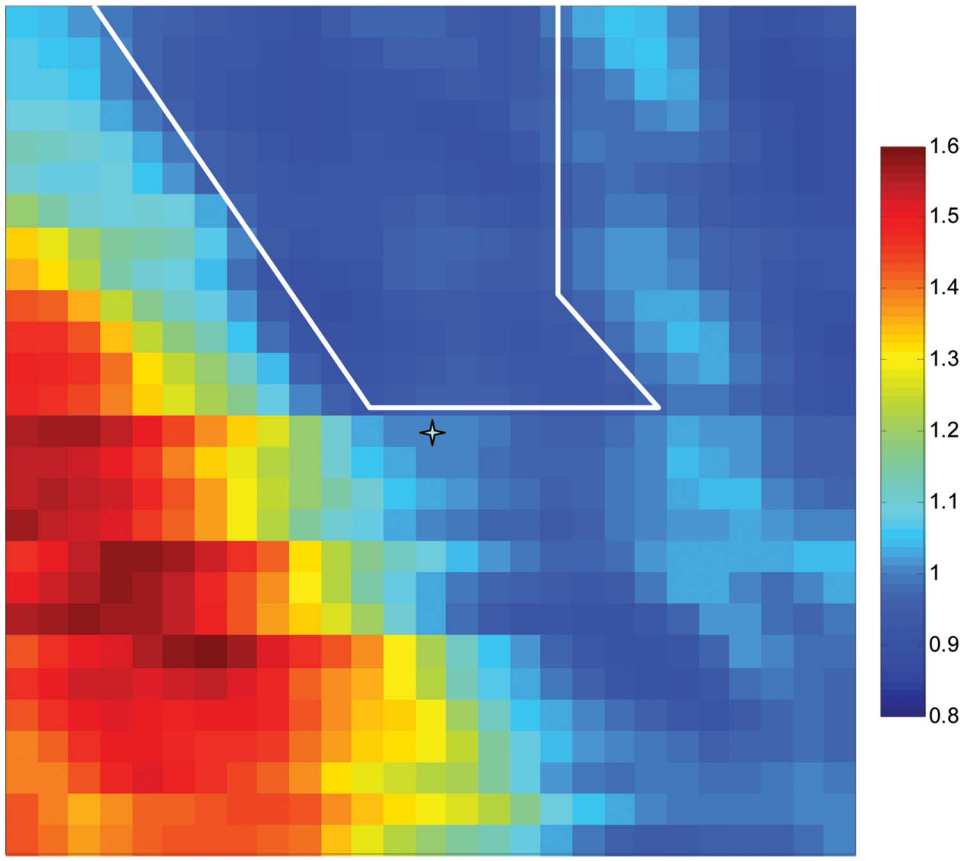

Fig. 13. Map of the annual standard deviation of the Tb measured at 6.9 GHz. The white line indicates the area recommended for the calibration of satellite sensors. The star indicates the Concordia station.

TABLE I
MODEL INPUT PARAMETERS

N. of Layers	Layers thickness (m)	Density (Kg/m^3)	Temperature	Grain radius (mm)
600	0.1 –1.5 (deepest layers)	0.314 – 0.92	(0-10 m): From experimental data down to 10 m : 54°C	(0-10 m): From experimental data $\sqrt{r_0^2 + \frac{K_{gr} \cdot depth}{\pi \cdot thickness}}$

past [10], with the exception of the 37 GHz channel where we estimated a higher value.

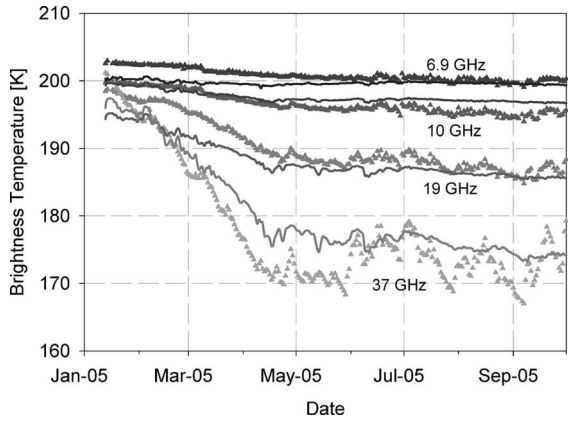

Fig. 14. Tb as a function of time: model simulations (continuous lines) compared with data taken from AMSR-E at V polarization (triangles).

V. CONCLUSION

The spatial and temporal variability of microwave emission from an area surrounding the Concordia base on the east Antarctic plateau has been studied using data from AMSR-E corroborated by snow measurements and model analysis.

Our analysis of the experimental data has shown that the emission at the lowest frequency (6.9 GHz) is quite uniform in time, is independent of surface temperature, and appears to be mostly influenced in space by snow morphology and topography and in time by snow temperature of the layers down to 4 m. On the other hand, emission at higher frequencies (19 and 37 GHz) is closely related to the seasonal variation in the surface layer temperature (the upper 2 m), while the spatial variability is due to different snow morphologies in these layers.

Model simulations were able to represent long-time series of satellite data and made it possible to identify the depth at which most radiation is emitted from the ice sheet at a certain frequency. In particular, at the lowest frequencies (6.9 and 10 GHz), the emission was mainly due to the snow layers down to 30 m, whereas at the highest frequencies (19 and 37 GHz), it was dominated by the layers of the first 10 m. The relatively small annual fluctuation in Tb at C-band was explained by the

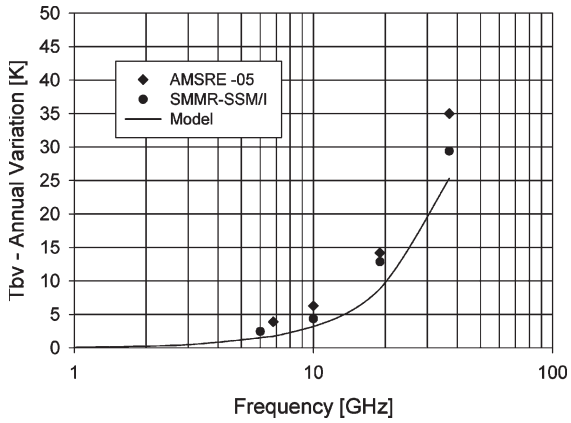

Fig. 15. Modeled and measured yearly variation (Tbmaximum–Tbminimum) in Tb as a function of frequency. Diamond: AMSR-E data 2005. Circle: Mean average value SMMR-SSM/I 1978–2000. Line: Model.

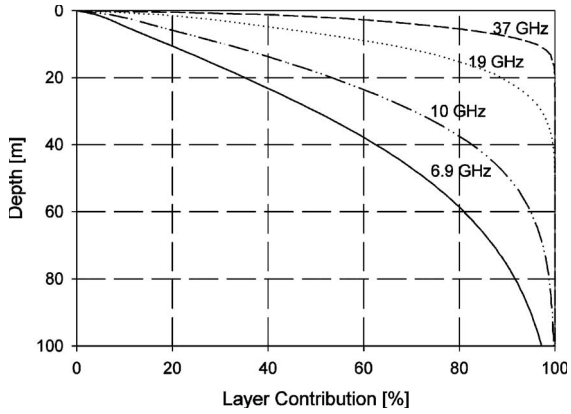

Fig. 16. Contribution of the snow layers to total emission at various frequencies between 6.9 GHz (C-band) and 37 GHz (Ka-band).

almost constant physical snow properties of the deeper layers assumed by the model.

From spatial and temporal analysis, this paper pointed out the portion of the investigated area that is more appropriate for use as an extended calibrator for spaceborne radiometers. Despite the fact that the AMSR-E frequency range does not extend to the L-band, we can assume, based on theoretical considerations and model simulation, that the Tb in the same area remains stable at this frequency as well and can then be useful for calibration of low-frequency missions, such as SMOS and Aquarius.

If the results obtained in the small area close to Concordia base are confirmed on a larger spatial scale (i.e., if other snow temperature data are available in other sites of the plateau), it will be possible to realize multitemporal maps of subsurface snow temperatures (down to 2 m) of the entire plateau. This would make a significant contribution to understanding the physical phenomena that regulate the snow deposition and air circulation of the plateau.

ACKNOWLEDGMENT

The authors would like to thank the Italian–French logistic team at Dome-C for their kind assistance during the experimental campaign and E. Salvietti of the University of Florence for his contribution to the collection of snow and temperature data during the winter period. Air temperature data were provided by the Antarctic Automatic Weather Stations Project (available at web site http://amrc.ssec.wisc.edu/). The authors would also like to thank the anonymous reviewers for their valuable comments.

REFERENCES

[1] H. J. Zwally, "Microwave emissivity and accumulation rate in polar firn," *J. Glaciol.*, vol. 18, no. 79, pp. 195–215, 1977.

[2] D. J. Cavalieri, J. P. Crawford, M. R. Drinkwater, D. T. Eppler, L. D. Farmer, R. R. Jentz, and C. C. Wackerman, "Aircraft active and passive microwave validation of sea ice concentration from the Defense Meteorological Satellite Program Special Sensor Microwave Imager," *J. Geophys. Res.*, vol. 96, no. C12, pp. 21 989–22 008, Dec. 1991.

[3] D. G. Long and M. R. Drinkwater, "Azimuth variation in microwave scatterometer and radiometer data over Antarctica," *IEEE Trans. Geosci. Remote Sens.*, vol. 38, no. 4, pp. 1857–1870, Jul. 2000.

[4] K. C. Jezek, C. J. Merry, and D. J. Cavalieri, "Comparison of SMMR and SSM/I passive microwave data collected over Antarctica," *Ann. Glaciol.*, vol. 17, pp. 131–136, 1993.

[5] C. J. Van der Veen and K. C. Jezek, "Seasonal variations in brightness temperature for central Antarctica," *Ann. Glaciol.*, vol. 17, pp. 300–306, 1993.

[6] M. Drinkwater, N. Floury, and M. Tedesco, "L-band ice sheet brightness temperatures at Dome C, Antarctica: Spectral emission modelling, temporal stability and impact of the ionosphere," *Ann. Glaciol.*, vol. 39, no. 1, pp. 391–396, Jun. 2003.

[7] D. P. Schneider and E. J. Steig, "Spatial and temporal variability of Antarctic ice sheet microwave brightness temperatures," *Geophys. Res. Lett.*, vol. 29, no. 20, p. 25-1, Oct. 2002.

[8] D. P. Schneider, E. J. Steig, and J. Comiso, "Recent climate variability in Antarctic from satellite-derived temperature data," *J. Clim.*, vol. 17, no. 7, pp. 1569–1583, Apr. 2004.

[9] I. Sherjal and M. Fily, "Temporal variations of microwave brightness temperatures over Antarctica," *Ann. Glaciol.*, vol. 20, pp. 19–25, 1994.

[10] S. Surdyk, "Using microwave brightness temperature to detect short-term surface air temperature changes in Antarctica: An analytical approach," *Remote Sens. Environ.*, vol. 80, no. 2, pp. 256–271, May 2002.

[11] G. Macelloni, M. Brogioni, P. Pampaloni, M. Drinkwater, and A. Cagnati, "DOMEX 2004: An experimental campaign at Dome-C Antarctica for the calibration of space-borne low-frequency microwave radiometers," *IEEE Trans. Geosci. Remote Sens.*, vol. 44, no. 10, pp. 2642–2653, Oct. 2006.

[12] M. Frezzotti, S. Gandolfi, F. La Marca, and S. Urbini, "Snow dune and glazed surface in Antarctica: New field and remote sensing data," *Ann. Glaciol.*, vol. 34, pp. 81–88, 2002.

[13] M. Frezzotti and O. Flora, "Ice dynamics features and climate surface parameters in east Antarctica from Terra Nova Bay to Talos Dome and Dome C: ITASE Italian traverses," *Terra Antartica*, vol. 9, no. 1, pp. 47–54, 2002.

[14] S. R. Hudson and R. E. Brandt, "A look at the surface-based temperature inversion on the Antarctic plateau," *J. Clim.*, vol. 18, no. 11, pp. 1673–1696, Jun. 2005.

[15] D. Six, M. Fily, S. Alvain, P. Henry, and J. P. Benoist, "Surface characterization of the Dome Concordia area (Antarctica) as a potential satellite calibration site, using SPOT4/Vegetation instrument," *Remote Sens. Environ.*, vol. 89, no. 1, pp. 83–94, Jan. 2003.

[16] "Eight glacial cycles from an Antarctic ice core," *Nature*, vol. 429, no. 6992, pp. 623–628, Jun. 2004.

[17] Frezzotti *et al.*, "New estimations of precipitation and surface sublimation in East Antarctica from snow accumulation measurements," *Clim. Dyn.*, vol. 23, no. 7/8, pp. 803–813, Dec. 2004.

[18] M. R. Van den Broeke, "Spatial and temporal variation of sublimation on Antarctica: Results of a high-resolution general circulation model," *J. Geophys. Res.*, vol. 102, no. D25, pp. 29 765–29 778, 1997.

[19] C. Genthon and G. Krinnern, "Antarctic surface mass balance and systematic biases in general circulation models," *J. Geophys. Res.*, vol. 106, no. D18, pp. 20 653–20 664, Sep. 2001.

[20] S. C. Colbeck, E. Akitaya, R. Armstrong, H. Gubler, J. Lafeuille, K. Lied, D. McClung, and E. Morris, *International Classification for Seasonal Snow on the Ground*. Geneva, Switzerland: IAHS, 1990.

[21] M. B. Lythe and D. G. Vaughn, the BEDMAP Consortium, *BEDMAP Bed Topography of the Antarctic 1:10,000,000 scale, BAS (Misc) 9*, 2000, Cambridge, U.K.: British Antarctic Survey.

[22] J. Comiso, "Surface temperatures in the polar regions from Nimbus 7 temperature humidity infrared radiometer," *J. Geophys. Res.*, vol. 99, no. C3, pp. 5181–5200, Mar. 1994.
[23] M. A. Fahnestock, T. A. Scambos, C. A. Shuman, R. J. Arthern, D. P. Winebrenner, and R. Kwok, "Snow megadune fields on the east Antarctic plateau: Extreme atmosphere–ice interaction," *Geophys. Res. Lett.*, vol. 27, no. 22, pp. 3719–3722, Nov. 2000.
[24] M. B. Giovinetto, "Glaciological studies on the McMurdo–South Pole Traverse 1960–61," Ohio State Univ., Columbia, OH, Institute of Polar Studies Rep. 7, 1963.
[25] F. T. Ulaby, R. K. Moore, and A. K. Fung, *Microwave Remote Sensing: Active and Passive*, vol. 3. Dedham, MA: Artech House, 1986.
[26] A. W. Bingam and M. R. Drinkwater, "Recent changes in the microwave scattering properties of the Antarctic ice sheet," *IEEE Trans. Geosci. Remote Sens.*, vol. 38, no. 4, pp. 1810–1820, Jul. 2000.
[27] C. Mätzler, A. Wiesmann, J. Pulliainen, and M. Hallikainen, "Development of microwave emission models of snowpacks," *IEEE Geosci. Remote Sens. Soc. Newslett.*, vol. 6, pp. 18–25, 2000.
[28] C. Mätzler and A. Wiesmann, "Extension of the microwave emission model of layered snowpacks to coarse-grained snow," *Remote Sens. Environ.*, vol. 70, no. 3, pp. 317–325, Dec. 1999.
[29] A. Wiesmann, C. Fierz, and C. Mätzler, "Simulation of microwave emission from physically modeled snowpacks," *Ann. Glaciol.*, vol. 31, no. 1, pp. 397–405, Jan. 2000.
[30] J. A. Kong, *Electromagnetic Wave Theory*. New York: Wiley-Interscience, 1990.
[31] N. Floury, M. Drinkwater, and O. Witasse, "L-band brightness temperature of ice sheets in Antarctica: Emission modelling, ionospheric contribution and temporal stability," in *Proc. IGARSS*, 2002, pp. 2103–2105.
[32] M. Tedesco, G. Macelloni, and P. Pampaloni, "A study on Dome C, Antarctic: Stratigraphy and electromagnetic modelling," IFAC Internal Rep. RR/OST/10.30, 2003.
[33] L. Tsang and J. Kong, *Scattering of Electromagnetic Waves*. New York: Wiley, 2001.
[34] Y. Q. Jin, "Wave approach to brightness temperature from bounded layer of random discrete scatterers," *Electromagnetics*, vol. 4, pp. 323–341, 1984.

Giovanni Macelloni (M'07) received the degree in electronic engineering from the University of Florence, Florence, Italy, in 1993.

In 1994, he collaborated with the Institute of Research of Electromagnetic Waves, National Council of Research, Florence. In 1994, he won a Fellowship at Alenia Space, Rome, within the framework of the European Space Agency (ESA) project Multifrequency Imaging Microwave Radiometer (MIMR). In 1997, he was hired as a Researcher with the Earth Observation Department, Istituto di Fisica Applicata "Nello Carrara" (IFAC), Sesto Fiorentino, Italy. Within the activities of the group, he deals with the development and design of microwaves radiometers, the planning and execution of the experimental campaigns, and the interpretation of data. Within this context, he has participated, as person in charge of the IFAC instrumentation, in numerous international campaigns (SIR-C/X-SAR, NOPEX, STAAARTE-RESEDA, STAAARTE-FORMON, ENVISNOW). In 2004, he was the Project Manager of the ESA project "DOMEX," which includes an experimental campaign that was carried out at Dome-C Antarctica in 2004 for the calibration of microwave satellite radiometers using the Antarctic plateau as an extended target. In addition to his experimental activity, he is involved in the implementation of electromagnetic models for the characterization of scattering and emission from natural targets (water, ground, agricultural and forest vegetation, and snow). He has also served various academic and professional establishments both as an External Referee and/or External Examiner, and has been a Consultant for companies in Italy. He has published more than 20 peer-reviewed papers in international journals and books, and more than 60 in the Proceedings of international conferences. His research interests include passive and active microwave remote sensing as applied to soil, vegetation, and snow using satellite, airborne, and ground-based data.

Mr. Macelloni has served as Reviewer for many international journals.

Marco Brogioni (S'05) was born in Siena, Italy, in 1976. He received the degree in engineering from the University of Siena, Siena, in 2003. He is currently working toward the Ph.D. degree in remote sensing at the University of Pisa, Pisa, Italy.

Since 2004, he has been with the Istituto di Fisica Applicata "Nello Carrara," Consiglio Nazionale delle Ricerche, Sesto Fiorentino, Italy. He is currently a Visitor Student with the University of California, Santa Barbara. His research deals with passive and active microwave remote sensing applied to snow using satellite (Aqua, Envisat, Seawinds) and ground-based data and with the development of passive and active microwave modeling for the snowpack.

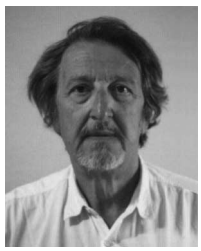

Paolo Pampaloni (M'86–SM'95–F'99) received the degree in electronic engineering from the University of Bologna, Bologna, Italy, in 1964.

He was a Visiting Scientist with the Institute of Radio Engineering (IRE), Russian Academy of Sciences, Moscow, Russia, in 1987 and 1989, and with the Massachusetts Institute of Technology, Cambridge, in 1999. He has been a Consultant for the European Space Agency (ESA) for microwave radiometry and member of the ESA Earth Observation Advisory Group (EOAC). He has served as Principal Investigator and Coinvestigator of several international projects and experiments in Europe and as Coordinator of numerous national and international research programs. He is currently with the Institute of Applied Physics, National Research Council, Florence, Italy. He is also an Adjunct Professor with The Electromagnetics Academy, Zhejiang University (TEA at ZJU), Hangzhou, China. He has published over 150 papers on international journal and conference proceedings and has edited three books with VSP Press. His current research deals with active and passive microwave remote sensing of land and, in particular, with the study of microwave emission and scattering from soil, snow, and vegetation.

Dr. Pampaloni is a member of Electromagnetic Academy (U.S.), the President of the Microwave Remote Sensing Center, and the Chairman of the IEEE Central and South Italy Section. He is the National Official Member of URSI Commission F (Wave Propagation and Remote Sensing). He has served as General Chairman of the 2nd and 6th Specialist Meetings on Microwave Radiometry and Remote Sensing (Florence 1988 and 1999). He was the General Chairman of the 15th International Geoscience and Remote Sensing Symposium (IGARSS'95) and was Guest Editor of the Special IGARSS'95 Issue of the IEEE TRANSACTIONS ON GEOSCIENCE AND REMOTE SENSING. Since 1994, he has been frequently involved in the Technical Program Committee of IGARSS. In addition, he has been Session Chairman and Organizer, as well as member of the technical program committees for numerous international conferences. He is an Associate Editor of the IEEE TRANSACTIONS ON GEOSCIENCE AND REMOTE SENSING. He received the IEEE GRSS Distinguished Achievements Award in 2004.

Anselmo Cagnati was born in Belluno, Italy, on October 26, 1956. He received the degree in forestry sciences in 1980.

Since 1981, he has been a Snow Scientist with the Centro Valanghe di Arabba, Agenzia Regionale per la Prevenzione e Protezione Ambientale del Veneto, Arabba di Livinallongo, Italy, where he is currently the Chief of the Meteo Office and Coordinator of Snow and Avalanche Service. Since 1994, he has participated in scientific expeditions in polar (Antarctica) and subpolar areas (Tierra del Fuego, Svalbard Islands) within the Antarctica National Research Program and the Arctic Strategic Project as Scientific Researcher and as Operating Unit Supervisor, mainly taking care of the analysis on snow physical properties and snow cover influence on permafrost. He is the author of various publications and over 70 articles related to snow and avalanches subjects published on scientific and divulgative reviews.